



Kinetic modeling of *Dodonaea viscosa* decomposition under microwave-assisted pyrolysis: A combined model-fitting and isoconversional approach

Safa W. Shakir ^{a, b, *}, Atheer M. Al-Yaqoobi ^b

^a Department of Chemical Engineering, College of Engineering, University of Tikrit, 34001, Iraq

^b Department of Chemical Engineering, College of Engineering, University of Baghdad, 10070, Iraq

Abstract

This work examines the kinetic behavior of *Dodonaea viscosa* during microwave-assisted pyrolysis as a means of addressing the limited insight regarding how biomass degradation pathways are affected by non-conventional heating. Thermogravimetric data were analyzed using both model-fitting (Coats–Redfern) and model-free (Friedman and Kissinger–Akahira–Sunose) methods to provide a thorough analysis. Results indicated that a third-order kinetic model appropriately described the general trend of decomposition; in contrast, iso-conversional analyses verified a multi-stage sequence with the activation energy declining during volatile yields and increasing at elevated conversion levels as a result of carbonaceous residue decomposition. These complementary understandings demonstrate that microwave-assisted heating ensures the development of characteristic reaction dynamics rather than those derived from traditional pyrolysis and thus supply mechanistic support for increased energy efficiency. The results not only unify methodology gaps between model-fitting and iso-conversional methodology but also provide useful direction for the optimization of microwave pyrolysis parameters, thus enhancing the sustainable production of lignocellulosic biomass-derived bioenergy.

Keywords: *Microwave-assisted pyrolysis; Dodonaea viscosa; Thermogravimetric analysis (TGA); Kinetic modeling; Isoconversional methods; Activation energy.*

Received on 27/09/2025, Received in Revised Form on 03/12/2025, Accepted on 03/12/2025, Published on 30/12/2025

<https://doi.org/10.31699/IJCPE.2025.4.16>

1- Introduction

The growing need for sustainable and renewable sources of energy prompted interest in biomass thermochemical conversion, in particular pyrolysis, for the production of biochar, bio-oil, and syngas due to lowered environmental impacts relative to fossil fuels [1]. The products thereof involve biochar, which is highlighted for porosity, extensive surface area, and active surface chemistry, facilitating a vast range of applications from soil amendment and heavy metal immobilization to wastewater treatment and catalysis [2, 3]. The nature of the biochar, however, depends mainly on the feedstock as well as the conversion technology. Typical pyrolysis systems involving external heat supply usually experience slow and tortuous heat transfer from the surface of particles to the core, which restricts energy efficiency [5, 6-8].

As a promising substitution strategy, microwave-assisted pyrolysis (MAP) takes advantage of the volumetric coupling of microwaves with polar molecules, leading to the acceleration of decomposition rates, the establishment of more even temperature profiles, and increased energy efficiency [9, 10]. Current research has indicated MAP increases the product yields, minimizes the pretreatment requirements, and optimizes the quality

of the resultant biochar, verifying the potential for large-scale applications for bio energies and the environment [11-15]. By a great margin, many of the researches carried out so far have been based on agricultural residues and woody biomass, without tapping into many idle sources of feeds. *Dodonaea viscosa*, a robust shrub indigenous to deserts and dry savanna environments, is a promising but untapped lignocellulosic biomass. The widespread growth, fast growth rates, and water resilience of this species render it a strong contender for biomass valorization for dryland ecosystems like Iraq [16, 17]. Nevertheless, the pyrolytic character of the biomass—most especially with microwave irradiation—has been comparatively unexplored.

Decomposition kinetics studies of the biomass would play a significant role in process parameterization, reactor development, as well as assessing the biomass as a renewable energy resource. Kinetic modeling offers valuable information on the multistage character of biomass decay [18-20]. Model-fitting techniques like the Coats–Redfern procedure provide reduced mechanistic explanations, whereas model-free (iso-conversional) techniques like Friedman and Kissinger–Akahira–Sunose (KAS) indicate activation energy distributions over conversion intervals, describing more intricate



*Corresponding Author: Email: eng.safawaleed@tu.edu.iq

© 2025 The Author(s). Published by College of Engineering, University of Baghdad.

This is an Open Access article licensed under a [Creative Commons Attribution 4.0 International License](https://creativecommons.org/licenses/by/4.0/). This permits users to copy, redistribute, remix, transmit and adapt the work provided the original work and source is appropriately cited.

degradative pathways [20-25]. A combination of the two ensures more accurate assessment of energy-dependent decay stages. Whereas the large body of studies on microwave-assisted pyrolysis since then focused on various agricultural wastes or wood-based biomass via model-based analysis as well as iso-conversional analysis alone [7, 12].

This article aims to not only target an insufficiently studied feedstock type in arid regions, *Dodonaea viscosa*, a type of desert shrub, but also combines dual-model analysis techniques (Coats-Redfern analysis model combined with Friedman/KAS analysis model) in a microwave-assisted environment. The two-approach strategy overcomes activation energy trends and mechanistic ambiguity, filling the research lacuna by employing overlooked desert biomass. Converting *Dodonaea viscosa* into valuable biochar, this study contributes to waste valorization plans and enriches the

portfolio of the sustainable lignocellulosic feedstocks for the production of bioenergy and catalysts.

2- Methodology

2.1. Feedstock preparation

Dodonaea viscosa biomass was collected from Tikrit University College of Engineering. The raw biomass was cleaned well by washing using deionized water for the removal of dust and impurities, followed by drying at 60 °C for 24 h using an oven until a constant weight was achieved. The dried biomass was also ground and sieved for the generation of a consistent size particle of 2.0–2.5 mm, a value selected for the avoidance of intraparticle heat transfer limitations during the pyrolysis process. The preparation steps are presented schematically as shown in Fig. 1 [16, 17].

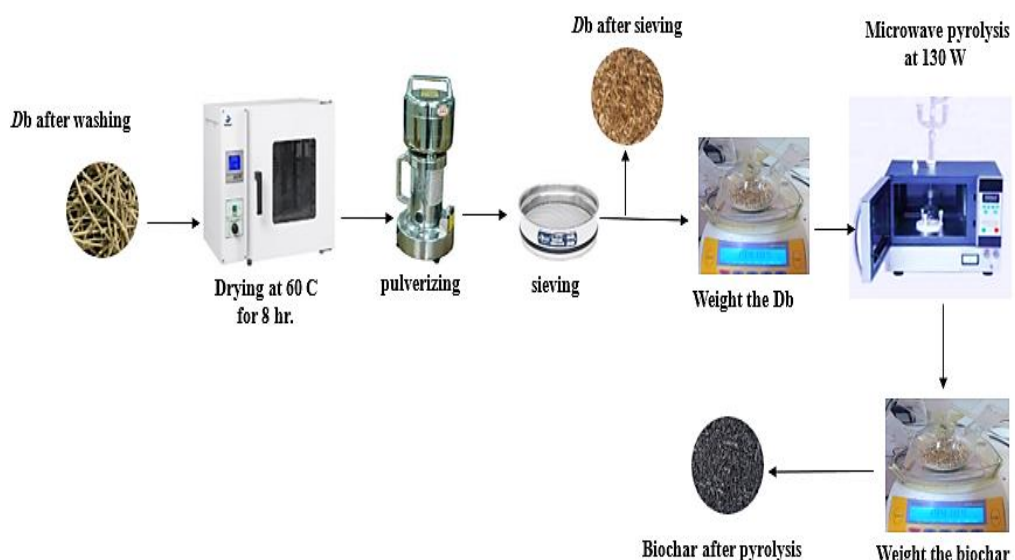


Fig. 1. The preparation steps of *Dodonaea viscosa*

2.2. Microwave-assisted pyrolysis system

Microwave pyrolytic experiments were carried out using a bench-scale microwave reactor (2.45 GHz, maximum power 1300 W; WBFY-205/ ZZKD / China). The reactor contained a quartz reactor tube and an infrared thermometer for real-time measurement of the temperature profiles. Prior to each experiment, the reactor was purged by high-grade nitrogen (99.99%) at a flow of 100 mL/min for the maintenance of an inert atmosphere and the prevention of the formation of secondary oxidation reactions. For each run, 10 g of the *Dodonaea viscosa* biomass was fed into the reactor. The microwave power remained at 130 W, as obtained from the preliminary optimum experiments. The growth of the temperature over time was monitored continuously, and the process ran for a time duration until the required

termination condition had been reached. Solid, liquid, and gaseous products were distinctly collected for later physicochemical characterization. A schematic diagram of the microwave pyrolysis system is shown in Fig. 2 [16, 17].

2.3. Thermogravimetric analysis

Thermal decomposition studies were carried out using a microwave reactor with a temperature sensor under a nitrogen atmosphere. Approximately 10 mg of sample was placed in a quartz reactor at 130 W for 25 min. [16]. The data, including weight loss (W_t) as a function of temperature and time, were used to calculate the degree of conversion (α) according to Eq. 1:

$$\alpha = \frac{W_i - W_t}{W_i - W_f} \quad (1)$$

Where: W_i is the initial weight of the sample (g), W_t is the weight of the sample at a given time (g) and W_f is the final mass of the sample (g).

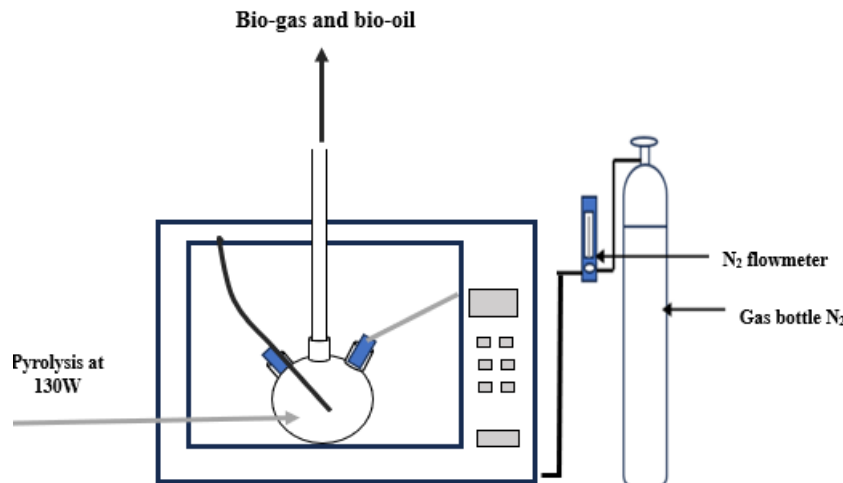
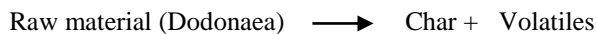


Fig. 2. Schematic diagram of microwave pyrolysis process

2.4. Kinetic modeling approaches

$$f(\alpha) = (1 - \alpha)^n \quad (5)$$

Kinetic parameters were determined with model-fitting and model-free processes: Solid-state kinetics may be investigated with thermal methods with the help of following the property of the sample during heat treatment or holding isothermally. Reaction kinetics was utilized during the present study with non-isothermal thermal data of a constant rate of heating [26, 27]. The pyrolytic reaction of the solid material might be described as follows:



The rate equation for the solid decomposition under isothermal conditions is as follows:

$$\frac{d\alpha}{dt} = k f(\alpha) \quad (2)$$

Where k is the rate constant of the reaction, $f(\sigma)$ is the function of σ and σ is the conversion or weight loss rate that can be calculated with the following equation.

The temperature dependent reaction constant k can be described with the Arrhenius law as given.

$$k = A e^{(-E/RT)} \quad (3)$$

Where T is the absolute temperature (K), R is the gas constant (8.3145 J mol⁻¹ K⁻¹), E is the activation energy (kJ/mol), and A is the pre-exponential or frequency factor (min⁻¹). The equation obtained from plugging Eq. 3 into Eq. 1 is as follows.

$$\frac{d\alpha}{dt} = A e^{(-E/RT)} f(\alpha) \quad (4)$$

$f(\alpha)$ can be proposed in the following form.

The following formula represents the heating rate as a function of time in non-isothermal experiments:

$$\frac{d\alpha}{dt} = \frac{d\alpha}{dt} \times \frac{dt}{dt} \quad (6)$$

The linear heating rate, β (K/min), for non-isothermal measurements can be expressed as follows:

$$\beta = \frac{dt}{dt} \quad (7)$$

Lastly, applying the linear heating rate Eq. 7 to Eq. 4 results in.

$$\frac{d\alpha}{dt} = \frac{A}{\beta} e^{(-E/RT)} f(\alpha)$$

or

$$\frac{d\alpha}{dt} = \beta \times \frac{d\alpha}{dt} = A e^{(-E/RT)} f(\alpha) \quad (8)$$

This equation is called the general equation of the rate of heating during non-isothermal experiments. The integrated reaction model or the so-called "integral function" or "temperature integral" is given by $G(\alpha)$, which is extracted from an integration and rearrangement of Eq. 8.

$$G(\alpha) = \int_0^\alpha \frac{d\alpha}{f(\alpha)} = \frac{A}{\beta} \int_0^T e^{(-E/RT)} dT \quad (9)$$

Many integral functions were suggested in the literature. The most common functions are summarized in Table 1. As per reports, accurate analytical solutions of the temperature integral are achieved through the use of nonlinear heating programs, like hyperbolic, parabolic, or non-Arrhenius temperature functions of the rate constant. This approach has never been utilized very commonly. This equation is known as the general equation of non-isothermal experiments, heating rate. Integration and recombination of Eq. 8 give.

Table 1. Various integral functions suggested in the literature

Mechanisms of the Reaction	$g(\alpha)$
Models of Chemical Reaction	
1st order	$-\ln(1 - \alpha)$
Reaction order ($n = 0.25, 1.5, 2, 3$)	$[(1 - \alpha)^{(1-n)} - 1]/(n - 1)$
Models of Diffusion Controlled	
1D transport – plane	α^2
2D transport	$\alpha + (1 - \alpha)\ln(1 - \alpha)$
3D transport – spherical (Jander)	$[1 - (1 - \alpha)^{(1/3)}]^2$
3D transport – (Anti-Jander)	$[(1 + \alpha)^{(1/3)} - 1]^2$
Models of Phase Boundary Reaction	
2D, shrinking cylinder	$1 - (1 - \alpha)^{(1/2)}$
3D, contraction of a sphere	$1 - (1 - \alpha)^{(1/3)}$
Models of Nucleation Reaction	
$n = 1, 1.5, 2, 3$ (Avrami–Erofeev)	$[-\ln(1 - \alpha)]^{(1/n)}$
Power law	A
Power law	$\alpha^{(1/2)}$
Power law	$\alpha^{(1/3)}$

The integration variable is then written in terms of the substitution of X in place of E/RT so as to present the above (4.9) integral in a more general expression, and the integration limit is then altered as:

$$G(\alpha) = \frac{AE}{\beta R} \int_x^{\infty} \frac{e^{-x}}{x^2} dx = \frac{AE}{\beta R} P(x) \quad (10)$$

In this case, the integral function has also been given the symbol p(x). There are a few alternative methods that can be applied to get the solution from this point. The next few sections clarify these methods. Table 2 also indicates each method and its main assumptions with the plotting methods.

2.4.1. Model-fitting method (Coats–Redfern)

This method was applied to determine the most suitable reaction order (n) and corresponding kinetic parameters (E, A). The integral form of the rate equation was linearized, and the best-fitting reaction order was identified based on correlation coefficient (R^2) values [24].

$$G(\alpha) = \frac{AE}{\beta R} P(x) \cong \frac{AE}{\beta R} \left[\frac{e^{-x}}{x^2} \left(1 - \frac{2!}{x} + \frac{3!}{x^2} - \frac{4!}{x^3} + \dots \right) \right] \cong \frac{AE}{\beta R} \left[\frac{e^{-x}}{x^2} \left(1 - \frac{2}{x} \right) \right] = \frac{ART^2}{\beta E} \left(1 - \frac{2RT}{E} \right) e^{-\frac{E}{RT}} \quad (11)$$

The G(α) expression can also now be written for most orders of reaction value.

When $n=1$, the function becomes $G(\alpha) = -\ln(1-\alpha)$, and when $n \neq 1$, it has the following expression:

$$G(\alpha) = 1/n - 1[(1 - \alpha)^{1-n} - 1] \quad (12)$$

These equations might be obtained by substituting the G(α) functions in equation (11) and rearranging them:

$$n = 1, \ln \left[-\frac{\ln(1 - \alpha)}{T^2} \right] = \ln \left[\frac{AR}{\beta E} \left(1 - \frac{2RT}{E} \right) - \frac{E}{RT} \right] \quad (13)$$

$$n \neq 1, \ln \left[-\frac{\ln(1 - \alpha)^{(1-n)}}{T^2(1-n)} \right] = \ln \left[\frac{AR}{\beta E} \left(1 - \frac{2RT}{E} \right) - \frac{E}{RT} \right] \quad (14)$$

For the determination of the reaction order, plotting method is generally applied. By linear fitting of the left-hand side of Eqs. 13 and 14 versus 1/T, the order of the reaction can be determined. In addition, for the best fitted reaction order, the kinetic parameters A and E can be calculated. As a result of plotting, the left-hand side of the equations versus 1/T gives straight lines. The highest R^2 values among these straight lines represent the best possible reaction order. By using the slope of these obtained straight lines (-E/R), the activation energy (E) of the process can be figured out. Also, by taking the temperature at which $W_t = (W_0 + W_f)/2$ in the place of T in the intercept term of Eqs. 12 and 13, the pre-exponential factor can be calculated [9].

2.4.2. Model-free methods (iso conversional)

In this study, two iso conversional (model-free) methods—the Friedman (differential) and Kissinger–Akahira–Sunose (KAS) (integral) approaches—were employed to estimate activation energy without assuming a specific reaction mechanism. These approaches are particularly recommended for biomass systems because they effectively capture variations in activation energy (E) across different degrees of conversion [9, 10]. While model-fitting methods can sometimes satisfactorily predict solid-state reaction kinetics, they often oversimplify complex processes such as biomass decomposition, where multiple reactions occur simultaneously [20, 27]. To overcome this limitation, model-free methods were developed on an iso conversional basis, assuming that the degree of conversion remains constant while the reaction rate constant (k) depends only on temperature. Among these, the Friedman method, one of the earliest iso conversional approaches [10], is applied by taking the natural logarithm of each side of Eq. 8.

$$\ln \left(\frac{d\alpha}{dt} \right) = \ln \left[\beta \left(\frac{d\alpha}{dt} \right) \right] = \ln [Af(\alpha)] - \frac{E}{RT} \quad (15)$$

Friedman's kinetic model also supposes that the f(α) function of conversion does not depend on time and, consequently, has an independent value, so the thermal degradation process does not depend on the temperature

and is described only by the rate of mass loss. The slope of the $\ln [\beta/\alpha]$ vs $1/T$ diagram, giving a straight line, is typically applied to define the activation energy [10]. But Kissinger and Akita and Sumiyoshi (KAS method) use another Doyle's approximation in the interval $20 \leq x \leq 50$ and suppose that α has an independent value. It can be described in the following way:

$$\log p(x) \approx \frac{\exp^{-x}}{x^2} \quad (16)$$

Substituting Eq. 16 into the temperature integral Eq. 10 provides the general equation of the KAS method:

$$\ln\left(\frac{\beta}{T_m^2}\right) = -\frac{E}{R}\left(\frac{1}{T_m}\right) - \ln\left[\left(\frac{E}{AR}\right)\int_0^\alpha \frac{d\alpha}{f(\alpha)}\right] \quad (17)$$

Where T_m is the temperature at the maximum reaction rate. The apparent activation energy can be obtained by plotting $\ln \beta$, T_m^2 vs $1/T_m$. The slope of the obtained straight lines gives the activation energy. Summary of the applied model-free, and model-fitting kinetic methods was presented in Table 2.

Table 2. An overview of the kinetics of model fitting and model free methods

Model-free approaches	Forms and Assumptions in General	The Plotting procedure
Friedman Method (differential Iso conversional)	$\ln \frac{d\alpha}{dt} = \ln[\beta] \frac{d\alpha}{dT} = \ln[A] f(\alpha) - \frac{E}{RT}$ assuming that $f(\alpha)$ stays constant. Degradation solely depends on the rate of mass loss and is not affected by temperature.	$\ln\left(\frac{d\alpha}{dt}\right)$ vs $(1/T)$ Slope = $-E/R$
Flynn–Wall–Ozawa Method (integral iso conversional)	Based on Doyle's approximation: $\log p(x) \approx -2.315 - 0.4567x$, for $20 \leq x \leq 60$ $\ln\beta = \log \frac{AE}{Rg(\alpha)} - 2.315 - 0.4567 \frac{E}{RT}$ assumes that throughout degradation, the apparent activation energy remains constant.	$\log\beta$ vs $(1/T)$ Slope = $-0.4567 \frac{E}{R}$
Kissinger–Akahira–Sunose Method (integral)	Based on Doyle's approximation: $\log p(x) \approx \exp\left(\frac{-x}{x^2}\right)$ for $20 \leq x \leq 50$ $\ln\frac{\beta}{T_m^2} = \frac{-E}{R} T_m - \ln\frac{E}{AR} \int_0^\alpha \frac{d\alpha}{f(\alpha)}$ Assumes α is fixed.	$\ln\frac{\beta}{T_m^2}$ vs $\frac{1}{T_m}$ Slope = E
Model fitting Approaches	$n = 1$, $ln\left[-\frac{\ln(1-\alpha)}{T^2}\right] = \ln\left[\frac{AR}{\beta E}\left(1 - \frac{2RT}{E}\right)\right] - \frac{E}{RT}$ $n \neq 1$, $ln\left[-\frac{\ln(1-\alpha)^{(1-n)}}{T^2(1-n)}\right] = \ln\left[\frac{AR}{\beta E}\left(1 - \frac{2RT}{E}\right)\right] - \frac{E}{RT}$ makes assumptions about the value of the reaction order and applies Taylor series expansion.	$\ln g(\alpha)$ vs $\frac{1}{T}$ Slope = $-\frac{E}{R}$ Intercept = $\ln\left[\frac{AR}{\beta E}\right]$

2.5. Rationale and limitations of kinetic models

This particular investigation uses model fitting (Coats-Redfern equation) as well as iso-conversional (Friedman, Kissinger-Akahira-Sunose-KAS) analysis techniques to quantify the *Dodonaea viscosa* pyrolysis reaction under microwave-assisted environments. This particular model is used as a rudimentary form of analysis that enables determination of a reaction order as well as a reaction activation enthalpy, attempting a first-order estimation of a broad decay process. This particular equation contains certain drawbacks in that a reaction model is considered as one process with a fixed reaction activation enthalpy over the entire process, neglecting possibly intricate multistage decay processes of a particular type of substrate such as lignocellulosic material in a microwave field [12].

To address this, iso-conversional techniques (Friedman and KAS) are used in this study, as they can generate values of the activation energy that vary with conversion independent of a fixed reaction model. Iso-conversional techniques evaluate well the dynamic changes in the values of activation energy linked to the stepwise decomposition of hemicelluloses, celluloses, and lignin in

the process of biomass pyrolysis [7]. However, iso-conversional techniques also possess certain drawbacks, as they only describe apparent pathways in terms of generation of values of activation energy independent of fixed reaction mechanisms in a process that could possess slightly negative values of E in differential techniques such as Friedman.

By employing a combination of both methods, the results benefit from the strengths of both, as the Coats-Redfern analysis yields a concise qualitative description of reaction order and kinetics, whereas the Friedman and KAS analyses describe conversion-dependent dynamics, thereby collectively providing a more holistic description of *Dodonaea viscosa* pyrolysis under microwave irradiation than either model alone. Moreover, employing dual modeling makes sure that overall tendencies as well as process-stage-specific details are both taken into account.

3- Discussion

3.1. The thermogravimetric studies (TGA) of *Dodonaea viscosa*

A significant variation in the range of decomposition temperatures as well as weight loss with increased microwave power (from 130 W to 650 W) is a significant sign that microwaves induce a notable variation in the thermal properties of *Dodonaea viscosa*. As shown in Fig. 3 at a less intensive power (from 130 W to 260 W), the initial weight loss (approximately 7-22 g) in the range of ~100-250°C is mostly contributed to by the elimination of moisture in addition to the initial decomposition of hemicelluloses. At more intensive power (390 W in the range of ~150-300°C, 520 W in the range of ~350-500°C, as well as in the range of ~450-850°C at the highest intensity of power (650 W)), a higher weight loss (about 10-29 g) is observed.

This conclusion is consistent with the observed phenomenon of microwave-assisted pyrolysis (MAP), suggesting that higher volume heating rates as well as elevated internal temperature rise result in earlier devolatilization processes as well as increased carbonization of chars produced [11, 12]. For example, results obtained by Fernández et al. suggest that microwave power influences the start of devolatilization as well as the production of char in the MAP pyrolysis of forest biomass. Again, Liu et al. suggest that higher microwave power is effective in improving the devolatilization process [11, 12].

This effect is observed in the presented data, as the "active" window of decomposition is shifted towards higher temperatures due to higher microwave power, thereby confirming that microwave power is effective in enhancing the pyrolysis process [12]. It is also important to highlight that this wider temperature range of 650 W (450-850°C) is a pointer that microwave pyrolysis is well into the lignin/char decomposition process, especially given that higher power intensities of microwaves trigger higher activation energies in the lignin-rich composition [7]. This significant variation in temperature range, as well as the substantial material loss, is a pointer that microwave pyrolysis not only accelerates the pyrolysis process, as highlighted in various previous discussions, but in fact allows a new reaction regime in the biomass sample.

3.2. Kinetic study by the Coats–Redfern

The Coats–Redfern analysis was presented in Fig. 4 and the calculated kinetic parameters are given in Table 3. It indicates the reaction order that best describes the overall decomposition process is approximately 3 ($R^2 \approx 0.94$), in which the activation energy (E) is a function of the reaction order (from approximately 12.7 kJ mol⁻¹ to 91.6 kJ mol⁻¹ as n increases from 0 to 3). This implies that the *Dodonaea viscosa* decay process in MAP is not a simple first- or second-order reaction since a higher reaction

order suggests a multiple-step process of decay (e.g., moisture/volatiles → cellulose → lignin/residue).

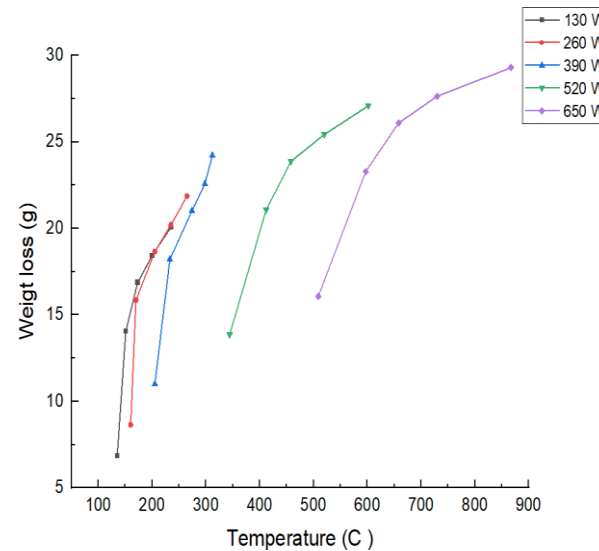


Fig. 3. The TGA of the microwave pyrolysis of *Dodonaea viscosa* for 25 min

At a comparable level of studying biomass under MAP, model-fitting approaches require a higher reaction order or a combination of reactions in fitting the multi-component characteristics of lignocellulosic materials [12]. With increasing values of reaction order in the given experiment, the dominating factor becomes evident, implying that the sample had a higher concentration of a compound that is less sensitive to higher temperatures, as evident under Lignocellulosic Materials [7]. Nevertheless, the drawback of the Coats–Redfern equation is that it enforces a fixed reaction mechanism (through the modelled reaction order). Moreover, this equation fails to account for the varying mechanisms that evolve during MAP pyrolysis as a result of differences in heat/mass transfer rates in MW rather than conventional heating. As already stated, MAP is expected to result in faster internal heating rates, thereby suggesting that modelling this process as a first-order reaction is a simplification [18, 28].

3.3. Iso-conversional (Model-Free) kinetic analysis

To overcome the limitation of model-fitting analysis, iso-conversional methods, i.e., Kissinger–Akahira–Sunose (KAS) and Friedman, were utilized to span a wide conversion range ($\alpha = 0.34–0.91$). Table 4 displays the calculated kinetic parameters and the corresponding fitting equations, while Fig. 5 and Fig. 6 display the corresponding plots. Both methods produced excellent correlations ($R^2 = 0.93–0.99$), and Friedman consistently produced higher values, justifying the adequacy of the study. Activation energies (E_a) had a strong dependence upon conversion, as one would expect for the multistep and complicated *Dodonaea viscosa* pyrolysis. Fig. 5 shows that at limited conversion ($\alpha = 0.34$), quite elevated apparent activation energies were revealed (61.7 kJ/mol

using Friedman and 54.7 kJ/mol using KAS). As negative values are uncommon, a similar anomaly for biomass

pyrolysis research by Kumar et al. and Yao et al. exists [22, 23].

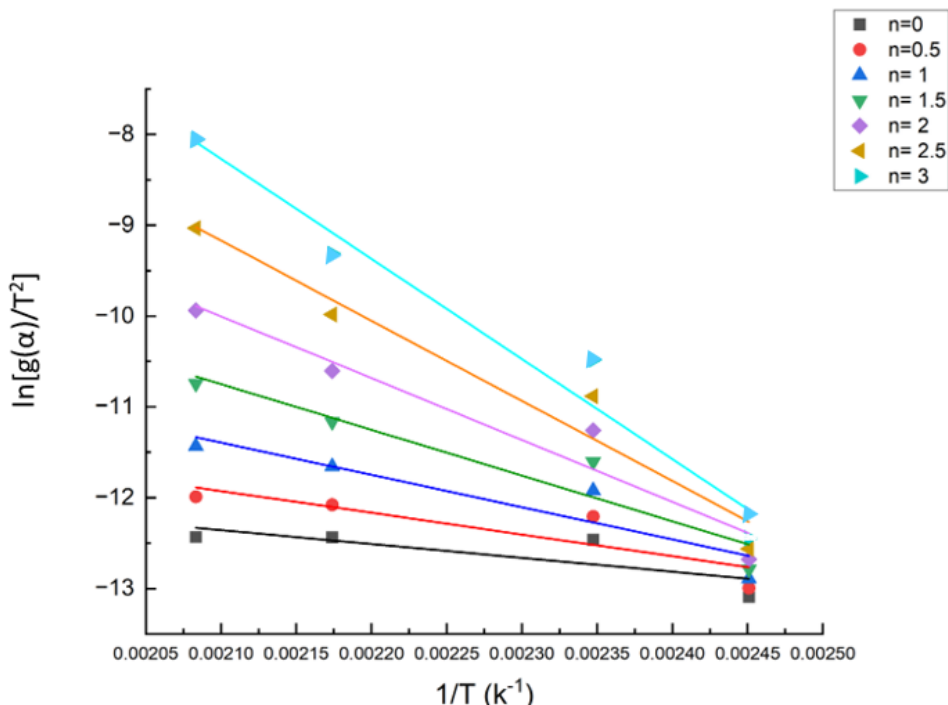


Fig. 4. The Coats-Redfern model for the pyrolysis of *Dodonaea viscosa*

Table 3. Calculated E (J/mol) and A (min⁻¹) values obtained from Coats-Redfern model for the pyrolysis of *Dodonaea viscosa*

Reaction 130 W			
n	R²	E (J/mol)	A (min⁻¹)
0	0.407	12691	326.47
0.5	0.618	19904.54	3072.72
1	0.76	29568.7	8791.87
1.5	0.849	41867.6	4021411.8
2	0.8987	56617	15987.018
2.5	0.925	73370.7	10.9 E+9
3	0.94	91611.96	3.22 E+12

The need to overcome strong cellulose–lignin bonds may explain the atypical results. With increasing conversion ($\alpha = 0.70$ – 0.84), activation energies lowered significantly (36.8 to 29.5 kJ/mol), suggesting the increasing favorability of decomposition due to the volatilization of hemicellulose and cellulose-derived volatiles. Similarly, reports indicated decreasing E value trends for agricultural byproducts like rice husk and corn stover [21, 23], where cellulose depolymerization dominates the mid-stage decomposition. When conversion became larger ($\alpha = 0.91$), activation energies rose once more, which agrees with the slow pace of

lignin-rich elements and char-forming components. This agrees with reports which emphasized lignin as the biomass element most thermally stable [20, 26]. In general, the activation energy values confirm *Dodonaea viscosa* pyrolysis proceeds through several stages, each governed by the relative reactivity of the biopolymers. The iso-conversional information confirms the pattern observed from other lignocellulosic biomass sources, thereby affirming the multistage mode of the degradation pathway and the suitability of *Dodonaea viscosa* as a model energy resource for thermochemical conversion.

Table 4. Calculated kinetic parameters, R² values and fitted equations from Friedman and KAS models (E, kJ/mol)

α	Friedman			KAS		
	Fitted equation	R²	E	Fitted equation	R²	E
0.34	y= -7418.6x +19.4	0.944	61678.2	Y= -6584.2+5.339	0.929	54741
0.7	y= -4429.9x+11.58	0.99	36830.18	Y= - 3544.8+2.6	0.986	29471.5
0.84	y= -8176.6x+ 18.98	0.959	67980.25	Y= - 7236.6 +4.68	0.948	60165.1
0.91	y= -6590.3x+14.929	0.978	54791.75	Y = - 5602.7 + 0.524	0.969	46580.8

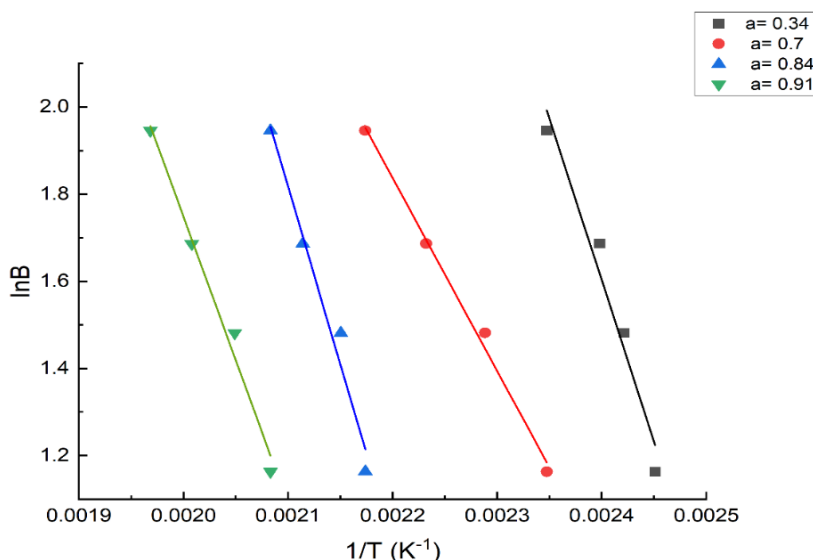


Fig. 5. Plots for Friedman kinetic models

On the other hand, Fig. 6 shows the Kissinger–Akahira–Sunose (KAS) model plots of $\ln(B/T^2)$ versus $1/T$ at different conversion levels ($\alpha = 0.34, 0.70, 0.84$, and 0.91), where each dataset forms a linear relationship, confirming the validity of the KAS iso conversional method for determining activation energy without assuming a reaction mechanism. The slopes of the straight lines correspond to $-E_a/R$, and their variation with conversion highlights the dependence of activation energy on the extent of decomposition.

At low conversion ($\alpha=0.34$), the steeper slope indicates a higher activation energy, suggesting that the initial bond-breaking stage requires more energy. With increasing conversion ($\alpha=0.70$ and 0.84), the slopes decrease, reflecting lower activation energies likely associated with the breakdown of less stable intermediates and the release of volatiles. At high conversion ($\alpha=0.91$), the slope becomes steeper again, pointing to the decomposition of more stable, carbonaceous residues that demand higher energy input. Overall, the KAS plots demonstrate that the thermal degradation is a multi-step process with variable activation energy across different reaction stages, consistent with complex decomposition pathways.

3.4. Comparison between Friedman and KAS results

Fig. 7 shows a comparison of the activation energy (E_a) obtained from Friedman analysis and Kissinger–Akahira–Sunose (KAS) iso-conversional analysis of *Dodonaea viscosa* pyrolysis. In both analyses, a converging trend in activation energy was observed that gradually diminished with a rise in conversion until mid-conversion ($\alpha \approx 0.5–0.8$), followed by a sharp increase at higher conversions. This trend is in accordance with the sequential thermal decomposition of hemicellulose, cellulose, and lignin components of the sample, as expected in the multicomponent composition of lignocellulosic biomass [21–24]. A depletion in E_a values in the mid-conversion

region can be ascribed to the facile depolymerization of cellulose as well as hemicellulose components, while the sharp increase in values at higher conversions is ascribed to the higher thermal stability of the lignin-based chars [22].

A slightly negative or varying E_a pattern observed in the Friedman results at lower conversions can be ascribed to the differential nature of the Friedman analysis and greater sensitivity to experimental error, observed earlier by Yao et al. in other microwave-assisted systems involving biomass [23]. However, a high degree of conformity between the iso-conversional results attests to the validity of the kinetic results. A combination of model fitting analysis (Coats-Redfern method) and model-free analyses (Friedman & KAS methods) produces a compounded analysis that is beneficial in understanding the reaction in a composite way in terms of reaction order [7, 12].

Collectively, these results verify that the sequential process of *Dodonaea viscosa* pyrolysis is governed by the steps of moisture evaporation, hemicellulose volatilization, cellulose depolymerization, and lignin carbonization. Therefore, this dual-model strategy allows for a holistic analysis of the kinetics of microwave-assisted biomass pyrolysis, as supported by recent analyses that resulted in a multistage model of biomass pyrolysis [23–25].

3.5. Integration of kinetic models and TGA behavior: Implications for MAP of *Dodonaea viscosa*

A clear pattern emerges of the TGA data with the results obtained from kinetic analysis: *Dodonaea viscosa* decomposition under microwave irradiation is accelerated in higher temperature regions as power levels escalate; kinetic analysis shows the process follows a third-order reaction in a general sense, with iso-conversional analysis indicating that reaction mechanisms change with conversion. Initial regions promote the release of low-

energy volatiles, intermediate regions promote cellulose decomposition (lower E), and the latter regions require greater external power input to induce lignin/char decomposition.

This pattern is in agreement with accelerated heating as well as greater internal temperature uniformity achievable in MAP [11,12]. Practically, such an arrangement means that in process optimization of MAP in *Dodonaea viscosa*, one needs to be aware of the differences in operating—

lower microwave power can be sufficient in the volatile extracts phase and primary fractionation, while higher power is required in secondary (char/graphitic residues) decomposition. Furthermore, the increase in the temperature of decomposition with higher microwave power indicates that microwave power level is a key factor that defines product output (biochar vs. volatiles), as already indicated by various reports in the literature [7].

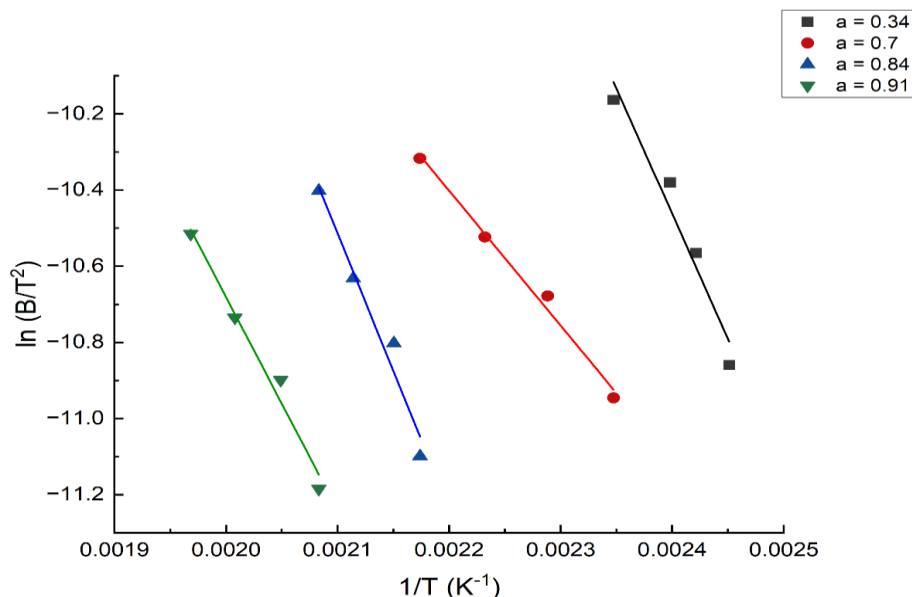


Fig. 6. Plots for KAS kinetic models

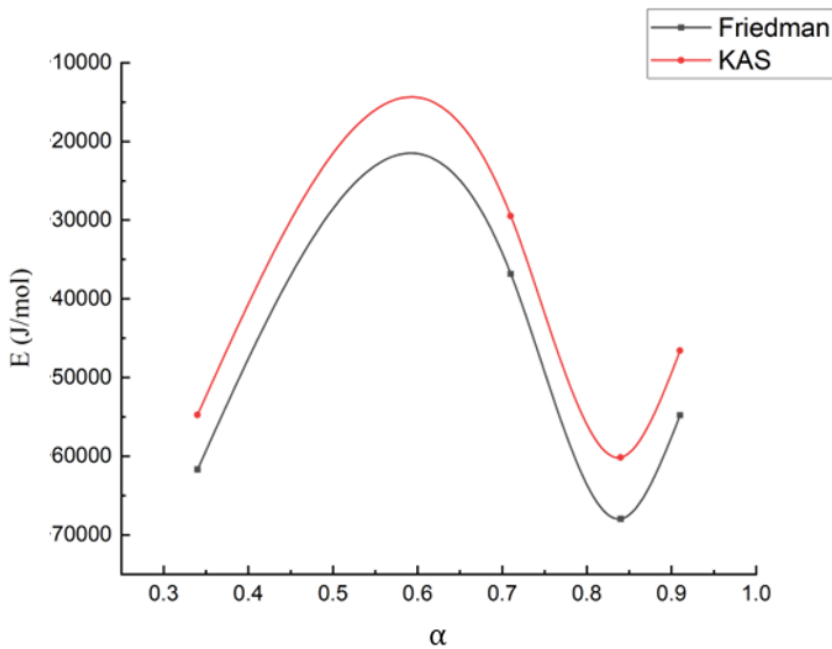


Fig. 7. Comparison of kinetic parameters derived from model-free methods

3.6. Comparison with conventional pyrolysis and contributions to literature

Compared to conventional external heating pyrolysis, microwave-assisted pyrolysis has distinct heating

dynamics in terms of faster internal heating, enhanced heat transfer, and possibly increased heating rates, resulting in differences in decomposition kinetics and yields [11, 12]. The results will provide new specific data in support of *Dodonaea viscosa*, a drought-tolerant desert

shrub, thereby increasing the range of MAP studies to new kinds of commercial wastes in addition to agricultural wastes. As indicated in the Introduction, most studies on MAP concern either forest biomass or agricultural wastes [6, 11]. This study fills a gap in existing literature by providing kinetic characteristics and TGA data on *Dodonaea viscosa* at various microwave power levels.

4- Conclusions

This article offers a holistic analysis of the kinetics of *Dodonaea viscosa* during microwave pyrolysis procedures, making use of TGA analysis techniques such as model-based analysis (Coats-Redfern equation analysis), as well as iso-conversional methods (Friedman and KAS methods). It has been revealed from TGA analysis that with increased intensity of microwave power, the decomposition of *Dodonaea viscosa* becomes faster, implying that microwave power is effective in degrading biomass. Also, the kinetics revealed that the overall reaction is of the third-order reaction type, whereas the iso-conversional analysis revealed that the process is a multistage reaction where the values of activation energy reduce during the liberation of volatile components of *Dodonaea viscosa*, as well as increase during the decomposition of the lignin part. These outcomes verify that microwave-assisted pyrolysis catalyzes a group of reaction dynamics that vary from those of conventional pyrolysis, offering a reaction model-based description of microwave-assisted thermal conversion of desert-suitable bioresources. Through the combination of model fitting techniques with iso-conversional techniques, this study offers a universal strategy towards microwave pyrolysis optimization that illustrates the efficiency of *Dodonaea viscosa* as a sustainable source of lignocellulosic material. Future studies could include reactor-scale experiments, as well as online analysis of the composition of the gases emitted during microwave pyrolysis and microwave absorber/bioresource pretreatments.

Acknowledgment

This study was partially supported by College of Engineering, Baghdad University and the College of Engineering, Tikrit University, Iraq.

Nomenclature

Parameter notation	Parameter definition
A	is known as the pre-exponential or frequency factor (min^{-1})
E	is the activation energy (kJ/mol)
K	is the rate constant of the reaction (depend on the reaction order)
N	Order of the reaction
R	is the universal gas constant ($8.3145 \text{ J mol}^{-1}\text{K}^{-1}$)

T	is the absolute temperature (K)
T	Time (min.)
T_m	is the temperature at maximum reaction rate (K)
$f(\alpha)$	is the function of α and α is the conversion or weight loss rate
β (K/min)	non-isothermal measurements linear heating rate
$G(\alpha)$	is known the integrated reaction model, so called as the "integral function" or "temperature integral"
$p(x)$	also represents the integral function
W_i	is the initial weight of the sample (g)
W_t	is the weight of the sample at a given time (g)
W_f	is the final mass of the sample (g)
Dodonaea viscosa	Dodonaea viscosa
KAS	Kissinger-Akahira-Sunose
R^2	Square root

References

- C. Chen and Y. Zhang, "Adsorption of pesticides from aqueous solutions onto low-cost natural adsorbents: A review," *Environmental Pollution*, Vol. 265, 114913, 2020. <https://doi.org/10.1016/j.envpol.2020.114913>
- M. J. Ahmed, "Enhanced conversion of glycerol-to-glycerol carbonate on modified bio-char from reed plant," *Iraqi Journal of Chemical and Petroleum Engineering*, Vol. 20, No. 4, pp. 15–20, 2019. <https://doi.org/10.31699/IJCPE.2019.4.3>
- D. Xu, Y. Gao, Z. Lin, W. Gao, H. Zhang, K. Karnowo, ... S. Zhang, "Application of biochar derived from pyrolysis of waste fiberboard on tetracycline adsorption in aqueous solution," *Frontiers in Chemistry*, Vol. 7, 943, 2020. <https://doi.org/10.3389/fchem.2019.00943>
- S. S. Mahmood and A. M. Al-Yaqoobi, "Production of biodiesel by using CaO nano-catalyst synthesis from mango leaves extraction," *International Journal of Renewable Energy Development*, Vol. 13, No. 6, pp. 1025–1034, 2024. <https://doi.org/10.61435/ijred.2024.60469>
- S. S. Mahmood and A. M. Al-Yaqoobi, "Microwave assisted production of biodiesel using CaO nano-catalyst produced from mango fallen leaves extract," *Journal of Ecological Engineering*, Vol. 26, No. 1, 2025. <https://doi.org/10.12911/22998993/195650>
- L. Dai, N. Zhou, H. Li, W. Deng, Q. Xiong, L. Dong, ... Y. Liu, "Recent advances in microwave-assisted catalytic conversion of biomass for biofuel production," *Chemical Engineering Journal*, Vol. 390, 124642, 2020. <https://doi.org/10.1016/j.cej.2020.124642>

[7] S. Syed, K. Mahmud, and J. Han, "Model-free kinetic modeling and thermochemical evaluation of biomass pyrolysis for sustainable energy recovery," *Journal of Analytical and Applied Pyrolysis*, Vol. 171, 2023. <https://doi.org/10.1016/j.jaat.2023.105993>

[8] T. R. Brazil, M. Gonçalves, E. G. dos Anjos, M. S. de Oliveira Junior, M. C. Rezende, "Microwave-assisted production of activated carbon in an adapted domestic oven from lignocellulosic waste," *Biomass Conversion and Biorefinery*, Vol. 14, 255-268, 2024. <https://doi.org/10.1007/s13399-021-02192-4>

[9] R. Bayón, R. García-Rojas, E. Rojas, and M. M. Rodríguez-García, "Assessment of isoconversional methods and peak functions for the kinetic analysis of thermogravimetric data and its application to degradation processes of organic phase change materials," *Journal of Thermal Analysis and Calorimetry*, Vol. 149, No. 23, pp. 13879–13899, 2024. <https://doi.org/10.1007/s10973-024-13494-w>

[10] B. Janković, V. Dodevski, F. Veljković, M. Janković, and N. Manić, "Application of model-free and model-based kinetic methods in evaluation of reactions complexity during thermo-oxidative degradation process: Case study of [4 (hydroxymethyl) phenoxyethyl] polystyrene resin," *Fire*, Vol. 7, No. 5, 165, 2024. <https://doi.org/10.3390/fire7050165>

[11] I. Fernández, S. F. Pérez, J. Fernández-Ferreras, and T. Llano, "Microwave-assisted pyrolysis of forest biomass," *Energies*, Vol. 17, No. 19, 2024. <https://doi.org/10.3390/en17194852>

[12] T. Emiola-Sadiq, L. Zhang, A. K. Dalai, "Thermal and kinetic studies on biomass degradation via thermogravimetric analysis: a combination of model-fitting and model-free approach," *ACS omega*, Vol. 6, 22233-22247, 2021. <https://doi.org/10.1021/acsomega.1c02937>

[13] M. F. Abd and A. M. Al-Yaqoobi, "The feasibility of utilizing microwave-assisted pyrolysis for Albizia branches biomass conversion into biofuel productions," *International Journal of Renewable Energy Development*, Vol. 12, No. 6, 2023. <https://doi.org/10.14710/ijred.2023.56907>

[14] M. F. Abd and A. M. Al-Yaqoobi, "The potential significance of microwave-assisted catalytic pyrolysis for valuable bio-products driven from Albizia tree," *Applied Science and Engineering Progress*, Vol. 18, No. 1, pp. 7454–7454, 2025. <https://doi.org/10.14416/j.asep.2024.07.016>

[15] M. F. Abd, A. M. Al-Yaqoobi, and W. S. Abdul-Majeed, "Catalytic microwave pyrolysis of Albizia branches using Iraqi bentonite clays," *Iraqi Journal of Chemical and Petroleum Engineering*, Vol. 25, No. 2, pp. 175–186, 2024. <https://doi.org/10.31699/IJCPE.2024.2.16>

[16] S. W. Shakir and A. Al-Yaqoobi, "Parametric and characteristic evaluation of microwave-assisted pyrolysis for the generation of biochar from Dedonea branches," *International Journal of Renewable Energy Development*, 2025. <https://doi.org/10.61435/ijred.2025.61186>

[17] S. W. Shakir and A. M. Al-Yaqoobi, "A modification of biochar surface functionalization and properties through catalyzed microwave pyrolysis of Dedonea branches," *Journal of Advanced Research in Fluid Mechanics and Thermal Sciences*, Vol. 132, No. 1, pp. 175–191, 2025. <https://doi.org/10.37934/arfmts.132.1.175191>

[18] D. K. Ojha, D. Viju, and R. Vinu, "Fast pyrolysis kinetics of lignocellulosic biomass of varying compositions," *Energy Conversion and Management*, X, Vol. 10, 100071, 2021. <https://doi.org/10.1016/j.enconman.2020.100071>

[19] H. Chen, J. Wang, and Q. Liu, "Iso-conversional kinetic analysis of rice husk pyrolysis using Friedman and KAS methods," *Fuel*, Vol. 312, 122980, 2022. <https://doi.org/10.1016/j.fuel.2021.122980>

[20] C. N. Arenas, M. V. Navarro, J. D. Martínez, "Pyrolysis kinetics of biomass wastes using isoconversional methods and the distributed activation energy model," *Bioresource technology*, Vol. 288, 121485, 2019. <https://doi.org/10.1016/j.biortech.2019.121485>

[21] Y. Chen, Q. Zhang, X. Li, and J. Liu, "Iso-conversional kinetic study of lignocellulosic biomass pyrolysis using model-free methods under microwave-assisted heating," *Energy Conversion and Management*, Vol. 267, 2022. <https://doi.org/10.1016/j.enconman.2022.115934>

[22] R. Kumar, R. Singh, and A. Verma, "Thermogravimetric and kinetic study of wheat straw pyrolysis: Iso-conversional approaches," *Renewable Energy*, Vol. 171, pp. 1332–1342, 2021. <https://doi.org/10.1016/j.renene.2021.03.067>

[23] D. Yao, Q. Hu, and H. Chen, "Understanding the anomalous activation energies in biomass pyrolysis via iso-conversional methods," *Energy Conversion and Management*, Vol. 221, 113170, 2020. <https://doi.org/10.1016/j.enconman.2020.113170>

[24] I. Najar, T. Rasool, "Optimization of multi stage Co-pyrolysis process using municipal solid waste and sawdust blends: A hybrid approach using iso-conversional modeling and machine learning," *Journal of the Indian Chemical Society*, Vol. 102, 101605, 2025. <https://doi.org/10.1016/j.jics.2025.101605>

[25] V. O. Shikuku, & T. Mishra, "Adsorption isotherm modeling for methylene blue removal onto magnetic kaolinite clay: a comparison of two-parameter isotherms". *Applied water science*, Vol. 11, No. 6, pp. 103, 2021. <https://doi.org/10.1007/s13201-021-01440-2>

[26] L. Zhang, J. Li, and Y. Sun, "Thermal degradation kinetics of lignin-rich biomass residues," *Journal of Analytical and Applied Pyrolysis*, Vol. 158, 105229, 2021. <https://doi.org/10.1016/j.jaap.2021.105229>

[27] K. Ling-Niao, G. Song-Tao, Y. Yang, and F. Feng, "Pyrolysis mechanism and pyrolysis kinetics of yellow wine lees," *RSC Advances*, Vol. 14, No. 24, pp. 16951–16959, 2024. <https://doi.org/10.1039/D4RA01541J>

[28] T. Qiu, C. Li, M. Guang, and Y. Zhang, "Porous carbon material production from microwave-assisted pyrolysis of peanut shell," *Carbon Research*, Vol. 2, No. 1, pp. 45, 2023. <https://doi.org/10.1007/s44246-023-00079-9>

النمذجة الحرارية لتحلل *Dodonaea viscosa* تحت التحلل الحراري بالموجات الدقيقة: منهج تكاملی يجمع بين النمذجة المعتمدة على المطابقة الإحصائية والطريقة الإيزو-كونفيريشنال

صفا ولید شاکر^{١، ٢، *}، اثیر محمد غالب^٢

١ قسم الهندسة الكيميائية، كلية الهندسة، جامعة تكريت، ٣٤٠٠١، العراق

٢ قسم الهندسة الكيميائية، كلية الهندسة، جامعة بغداد، ١٠٠٧٠، العراق

الخلاصة

تتناول هذه الدراسة السلوك الحراري لنبات *Dodonaea viscosa* أثناء التحلل الحراري بالموجات الدقيقة، وذلك لمعالجة محدودية الفهم المتعلق بكيفية تأثير مسارات تحلل الكتلة الحيوية بوسائل التسخين غير التقليدية. جرى تحليل بيانات التحليل الوزني الحراري باستخدام طريقتين: النمذجة المعتمدة على المطابقة (Coats)، والطريقة غير المعتمدة على نموذج محدد (Friedman، Redfern، Kissinger–Akahira–Sunose) بهدف تقديم تقييم شامل.

أظهرت النتائج أن نموذج التفاعل من الرتبة الثالثة يصف بشكل ملائم الاتجاه العام للتحلل، في حين أكدت التحليلات الإيزو-كونفيريشنال أن العملية تسير وفق آلية متعددة المراحل، حيث ينخفض طاقة التنشيط أثناء إطلاق المتطايرات، ثم ترتفع عند مستويات التحول الأعلى نتيجة تحلل البقايا الكربونية.

توضح هذه النتائج التكاملية أن التسخين بالموجات الدقيقة يحقق ديناميكيات تفاعل مميزة مقارنة بالتحلل الحراري التقليدي، مما يوفر دعماً ميكانيكياً لرفع كفاءة الطاقة. كما أن النتائج لا تسد الفجوة المنهجية بين الطريقتين فحسب، بل تقدم أيضاً توجيهياً عملياً لتحسين ظروف تشغيل المفاعلات العاملة بالتحلل الحراري بالموجات الدقيقة، وبالتالي تعزيز الإنتاج المستدام للطاقة الحيوية المشتقة من الكتلة الحيوية اللجنوسيلوزية.

الكلمات الدالة: التحلل الحراري بالموجات الدقيقة، التحليل الوزني الحراري (TGA)، النمذجة الحرارية، الطرق الإيزو-كونفيريشنال، طاقة التنشيط.